

FABRICATION, CHARACTERIZATION, TOXICITY AND BIOCOMPATIBILITY EVALUATION OF IRON OXIDE NANOPARTICLES

C. L. POPA^{a,b}, E. ANDRONESCU^c, M. STOICEA^d, P. LE COUSTOMER^e,
S. GALAUP^f, M. BEURAN^{d,g}, F. M. IORDACHE^{d,g}, A. TELCIAN^{h,i},
C. BLEOTU^j, A. M. PRODAN^{c,d,g,*}

^aNational Institute for Physics of Materials, P.O. Box MG 07, Bucharest, Magurele, Romania,

^bUniversity of Bucharest, Faculty of Physics, 405 Atomistilor Street, P.O. Box MG1, 077125, Magurele, Romania,

^cUniversity Politehnica of Bucharest, Faculty of Applied Chemistry and Materials Science, Department of Science and Engineering of Oxide Materials and Nanomaterials, 1-7 Polizu Street, P.O. Box 12-134, 011061 Bucharest, Romania,

^dEmergency Hospital Floreasca, Bucharest 5, Calea Floreasca nr 8, sector 1, Bucarest, Romania

^eUniversite Bordeaux, EA 4592 Géoresources & Environnement, EGID, 1 allée F. Daguin 18, 33607 Pessac Cedex France

^fENSEGID – IPB – EA 4592, 1 allée Daguin, 33607 Pessac, France

^gCarol Davila University of Medicine and Pharmacy, 8 Eroii Sanitari, sector 5, Bucharest, Romania

^hMicrobiology Department, Faculty of Biology, University of Bucharest, Aleea Portocalelor 1-3, 60101 Bucharest, Romania

ⁱS.C. Biotehnos S.A.

^jInstitute of Virology, Antiviral Therapy Department "Stefan S. Nicolau", 285 Mihai Bravu, 030304, Bucharest, Romania

The iron oxide nanoparticles were synthesized by an adapted coprecipitation method. Structural and morphological characterization of the obtained iron oxide nanoparticles were investigated by X-Ray Diffraction (XRD) and Transmission Electron Microscopy (TEM). Furthermore, *in vitro* and *in vivo* studies were investigated by cell viability assay and HeLa cells. For the analysis of iron oxide toxicity *in vivo*, several mice were treated with normal saline and iron oxide via intraperitoneal injection (IP). The XRD spectra showed the peaks associated to the spinel cubic lattice type with the lattice of 0.835 nm. By magnified TEM image, it could be observed that the samples have a uniform morphology with relatively spherical shape and nanometric size. Moreover, inverted fluorescence microscopy images of HeLa cells with normal phenotype and HeLa cells treated for 72 hours with a suspension of γ -Fe₂O₃ nanoparticles revealed the non-toxic character. The histopathological studies have demonstrated that at 72 hours after IP administration, the iron oxide nanoparticles are not accumulating in kidney and spleen, thus establishing their utility as drug delivery systems targeted to these organs.

(Received August 21, 2013; Accepted December 14, 2013)

Keywords: iron oxide, nanoparticles, cell viability, histopathological studies

*Corresponding author: alina.prodan@yahoo.co.uk

1. Introduction

The development of engineered nanoparticles has attracted a vivid interest in the recent years due to their outstanding properties[1-7]. One of the fields where the nanometric size of these particles had an important role is biomedicine[8-10].The increasing number of cancer cases is probably the most important public health issue of the last decades. The major challenges the researchers and clinicians are confronting with are the difficulty of early diagnosis and the appropriate therapy of cancerous tumors. Nowadays, the cancer treatment requires a large amount of drugs, and there is little control on their delivery system[11]. Thus, many healthy cells must be sacrificed in order to kill the cancerous ones, and the side effects of the treatment can sometimes be tremendous, making it very hard for the human body to recover. Scientists worldwide have focused their attention towards nanoparticles in order to improve the drug delivery systems, making them more accurate, and this way being able to reduce the adverse effects of the cancer drugs [12-13]. A type of nanoparticles which can be used for this purpose is represented by iron oxide nanoparticles, like magnetite (Fe_3O_4), or its oxidized form, maghemite ($\gamma\text{-Fe}_2\text{O}_3$)[14-15].

Previous studies have shown that iron oxide nanoparticles can be successfully used in different biomedical applications[16-18], such as MRI contrast agents [19], hyperthermia [20], tissue repairs, and targeted drug delivery[21]. In the field of cancer treatment, nowadays studies are concentrated on developing a drug delivery system based on iron oxide nanoparticles, the route towards the pathological site being controlled by aid of an external magnetic field, thus supplying the required amount of drugs to a more specific area, without destroying a large amount of healthy cells [21]. In order for this to be achieved, one of the properties which the iron oxide nanoparticles must have is a low cytotoxicity on the human cells. A good biocompatibility of the drug carrier decreases the chance to develop any adverse effects, making the treatment more efficient and improving the recovery time of the patient[22]. Another advantage of iron oxide nanoparticles is their ability to leave the bloodstream within a period of time less than 10 min, during which they have a great accumulation rate in different organs, 80-90% of the administered solution in the liver and 5-8% in the spleen [23], thus making the drug delivery process more precise.

The aim of this study was to obtain iron oxide nanoparticles by an adapted chemical coprecipitation method. The obtained iron oxide nanoparticles were investigated by X-ray diffraction (XRD) and transmission electron microscopy (TEM). The influence of iron oxide nanoparticles on HeLa cells was investigated, as well as their *in vivo* effects on mice, after intraperitoneal inoculation.

2. Materials and methods

2.1. Materials

Ferrous chloride tetrahydrate ($\text{FeCl}_2 \cdot 4\text{H}_2\text{O}$), ferric chloride hexahydrate ($\text{FeCl}_3 \cdot 6\text{H}_2\text{O}$), sodium hydroxide (NaOH), and hydrochloric acid (HCl) were purchased from Merck. De-ionized water was used in the synthesis of nanoparticles, and for rinsing of clusters.

2.2. Synthesis of iron oxide ferrofluid and characterization

The synthesis of iron oxide ferrofluid was carried out as reported in other papers [24-26]. The X-ray diffraction measurements for iron oxide samples were recorded using a Bruker D8 Advance diffractometer, with nickel filtered Cu K_α ($\lambda=1.5418 \text{ \AA}$) radiation, and a high efficiency one-dimensional detector (Lynx Eye type) operated in integration mode. The diffraction patterns were collected in the 2θ range $20^\circ - 70^\circ$, with a step of 0.02° and 34 s measuring time per step. Transmission electron microscopy (TEM) images for these samples were recorded using a FEI Tecnai 12 equipped with a low dose digital camera from Gatan. The specimen used for TEM investigations was prepared from suspensions. The nanoparticles were dispersed in deionized water and after that a droplet of supernatant was placed on a carbon-coated 200-mesh

copper grid. The sample were then dried at room temperature and attached to the sample holder on the microscope.

2.3. Cell viability assay

The quantification of cell viability was done using propidium iodide (PI) and fluoresceindiacetate (FdA). HeLa cells, (5×10^4) were seeded in each well of a plate with 24 wells and after 72 h were treated with a suspension of γ -Fe₂O₃ (200 μ l) nanoparticles diluted 100 times. The effects on cell viability were evaluated after 72 h by adding 100 μ L PI (0.1mg/mL) and 100 μ L FdA (0.1mg/mL) and fluorescence was quantified using a Observer D1 Carl Zeiss microscope. All cells from several fields were counted and cell viability was established by the ratio between viable (green) and dead cells (red)[27-28].

2.4. Animals

Male BalbC mice (weighing 300g) were purchased from the National Institute of Research and Development for Microbiology and Immunology "Cantacuzino", Bucharest. The mice were housed in an environment controlled for temperature ($22 \pm 2^\circ\text{C}$), light (12 h light/dark cycles) and humidity ($60 \pm 10\%$). The animals were maintained under specific pathogen free conditions in accordance with NIH Guide for the Care and Use of laboratory Animals

2.5. Histopathological examination

For analysis of iron oxide toxicity *in vivo*, the mice (n=4 per group) were treated with normal saline, iron oxide (2 mg/100 g) via intraperitoneal injection (IP). For histopathological examinations, selected organs (lung, spleen and kidney) were removed from the mice and fixed in 10% formalin. The organs were prepared as paraffin-embedded glass slides stained with hematoxylin and eosin. The morphological changes were observed under microscope[29].

3. Results and discussion

Fig. 1 shows the X-ray diffraction (XRD) patterns of the iron oxide nanoparticles obtained by an adapted chemical coprecipitation method. The obtained diffraction peaks at (220), (311), (400), (422), (511) and (440) are easily identified with the standard data for an fcc cubic maghemite structure. The XRD peaks displayed in Figure 1 can be indexed into the spinel cubic lattice type with the lattice of 0.835 nm. The value of the lattice parameter is in agreement with the values of the standard data (JCPDS no. 4-755).

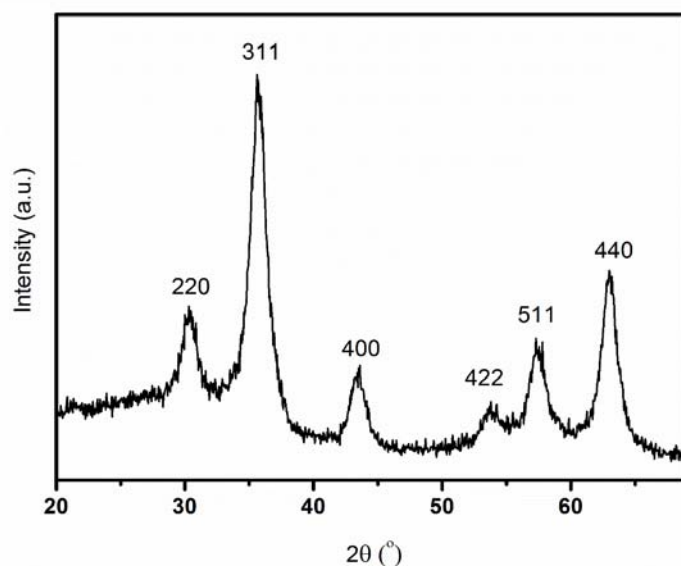


Fig. 1. XRD pattern of patterns of maghemite γ - Fe_2O_3 nanoparticles obtained by coprecipitation method.

The bright field TEM picture (Fig. 2) clearly showing that the samples obtained by coprecipitation method are composed of crystals with a relatively uniform, spherical morphology and a homogenous distribution. In the magnified TEM image Fig. 2 (B) it can be seen that the samples have a uniform morphology with relatively spherical shape and nanometric size.

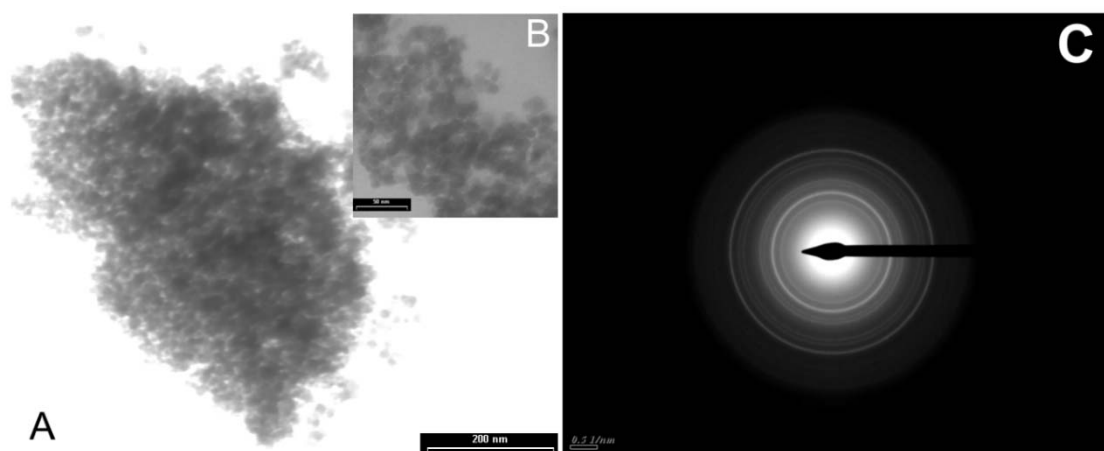


Fig. 2. Bright field TEM picture showing a homogeneous distribution of maghemite nanoparticles (A); Magnified TEM image of maghemite nanoparticles (B); SAED pattern from a region including a large number of maghemite nanoparticles (C).

Fig. 2 (C) presents the selected area electron diffraction (SAED) pattern recorded from an area containing a large number of well dispersed nanoparticles. The rings from the SAED pattern can be indexed as the (220), (311), (400), (422), (511) and (440) reflections of the cubic maghemite in agreement with. These results are in good agreement with the XRD results.

The toxicity and biocompatibility of the nanoparticles *in vitro* and *in vivo* need to be carefully evaluated before the material can be considered for medical applications [30,31].

The Fe_3O_4 nanoparticles proved to have satisfactory biocompatibility being appropriate for biomedical applications [32-34]. However, there are some reports on the capacity of iron oxide nanoparticles to induce the formation of free hydroxyl radical species, inhibiting cellular function and proliferation [35]

Inverted microscopy was used to observe the general morphological changes of HeLa cells treated with a suspension of $\gamma\text{-Fe}_2\text{O}_3$ (50mg/10ml) nanoparticles diluted 100 times (B), as compared to the control sample (A). The HeLa cells exhibited normal features, such as polygonal shape, homogeneous staining, and no cell fragments after exposure to iron oxide nanoparticles suspension. After a period of 72 hours, a large number of living cells could be observed (similar to the number of viable cells from the control sample), in the case of a suspension of $\gamma\text{-Fe}_2\text{O}_3$ (50mg/10ml), the number of dead HeLa cells (colored in red by propidium iodide) being very low, with a percentage less than 1%, proving that maghemitenanoparticles did not exhibit a cytotoxic effect on HeLa cells.

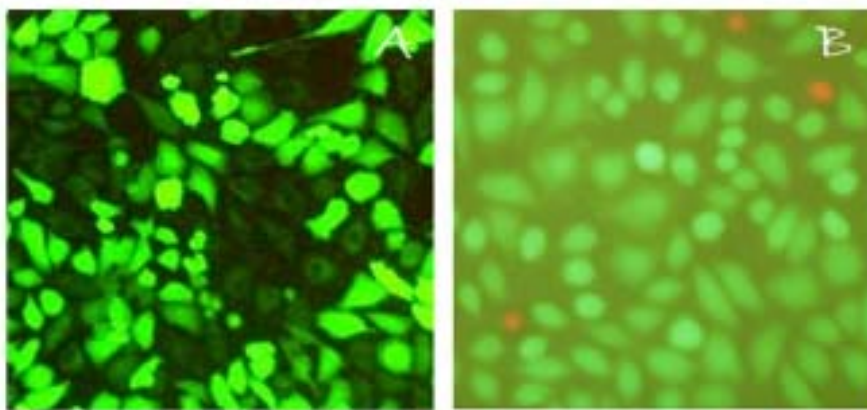


Fig.3. Inverted fluorescence microscopy images of HeLa cells with normal phenotype (A) and HeLa cells treated for 72 hours with a suspension of $\gamma\text{-Fe}_2\text{O}_3$ (50mg/10ml) nanoparticles (B).

Despite a considerable number of studies focused on the synthesis, characterization and coating of iron oxide nanoparticles for obtaining optimal parameters for different medical applications, the development of optimized *in vivo* biocompatibility assays ensuring their safe clinical use is still at the beginning [36,37].

Therefore, besides *in vitro* cytotoxicity assay on HeLa cells, the evaluation of nanoparticles toxicity in mice was used in this research.

Comparative cytoplasmic and nuclear details obtained on sections of organs harvested from the control animal batch (left column) and respectively, from the treated animals, 72 hours after the systemic intraperitoneal injection of iron oxide (right column) are shown in Figure 4. If we consider the lung, we can observe that the nuclei have enlarged volumes, unobtrusive anisomorphism and obvious nuclear anisochromia associated with the formation of nucleoli and binucleation. These features are comparable in both images (right and left). In the kidneys, we can observe the presence of tubular cells with nuclear and cytoplasmic anisochromia and granular degeneration (right image). Moreover, the right image depicts an area of architectural disarray and cells with pronounced nuclear and cytoplasmic anisomorphism. Vacuolar degeneration of the cytoplasm (right image) is also noted. Histopathological evaluation of the splenic tissue show nuclear contour irregularities, binucleations, mono- and binucleations (right image).

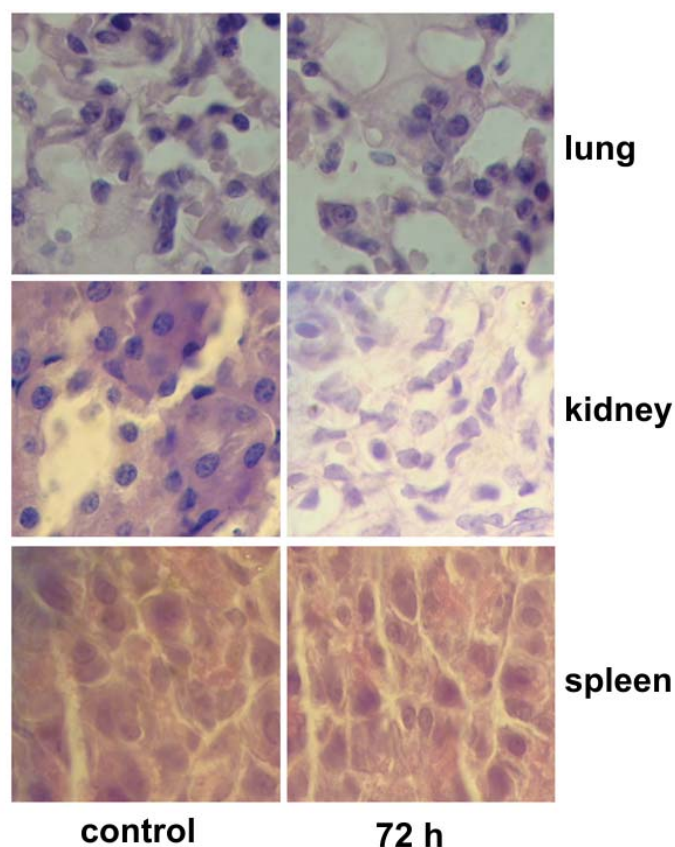


Fig.4. Comparative cytoplasmic and nuclear details made on sections of organs taken from the standard specimen (left column) and from a specimen after 72 h from the systematic injection of iron oxide suspension (right column).

These results are demonstrating that at 72 hours after IP administration, the iron oxide nanoparticles are not accumulating in kidney and spleen, demonstrating their utility as drug delivery systems targeted to these organs. However a significant amount of research still needs to be done in order to understand the long-term pharmacokinetic of these nanoparticles and the associated delayed toxicity.

4. Conclusions

The iron oxide nanoparticles prepared using an adapted coprecipitation chemical method presented a relatively spherical shape and nanometric size. The XRD investigations revealed that the as prepared iron oxide nanoparticles present the crystalline form of the cubic maghemite. The TEM images showed well crystallized materials having a nanometric size and spherical shape, without particle agglomeration. The obtained iron oxide nanoparticles are non-toxic, biocompatible and safe, as revealed by our *in vitro* and *in vivo* assays, proving a huge potential to be used in the next generation of diagnostic and therapeutic agents, improving the survival rate and the quality of life for many cancer patients.

References

- [1] A. Groza, A. Surmeian, M. Ganciu, I.I. Popescu, *Europhysics Letters*. **68**, 652 (2004).
- [2] A. Groza., M. Ganciu-Petcu, A. Surmeian, I.I. Popescu, *Mol.Cryst&Liq.Cryst.* **416**, 217 (2004).
- [3] A. Groza., A. Surmeian, M. Ganciu, R. Medianu, I.I. Popescu, *J. Optoelectron. Adv. Mater.* **7**, 2159 (2005).

- [4] A. Groza, A. Surmeian, M. Ganciu, R. Medianu, I. I. Popescu, J. Optoelectron. Adv. Mater. **7**, 2545 (2005).
- [5] A. Groza, A. Surmeian, C. Diplasu, M. Ganciu, P. Chapon, I. I. Popescu, J. Optoelectron. Adv. Mater. **12**, 2311 (2010).
- [6] A. Groza, A. Surmeian, C. Diplasu, C. Luculescu, P. Chapon, A. Tempez, M. Ganciu, Surface & Coatings Technology **212**, 145 (2012).
- [7] A. Groza, Romanian Reports in Physics **64**, Supplement, 1227 (2012).
- [8] S. L. Iconaru, A. M. Prodan, M. Motelica-Heino, S. Sizaret, D. Predoi, Nanoscale Res. Lett **7**, 576 (2012).
- [9] A. Figuerola, R. Di Corato, L. Manna, T. Pellegrino, Pharmacol. Res. **62**, 126 (2010).
- [10] R. R. Qiao, C. H. Yang, M. Y. Gao, J. Mater. Chem. **19**, 6274 (2009).
- [11] S. L. Iconaru, A. M. Prodan, P. Le Coustumer, D. Predoi, Journal of Chemistry, **2013**, 412079 (2013).
- [12] R. Langer, Nature **392**, 6679 (1998).
- [13] S. L. Iconaru, E. Andronescu, C. S. Ciobanu, A. M. Prodan, P. Le Coustumer, D. Predoi, Dig J Nanomater Bios **7**, 399 (2012).
- [14] D. Predoi, C. S. Ciobanu, M. Radu, M. Costache, A. Dinischiotu, C. Popescu, E. Axente, I. N. Mihailescu, E. Gyorgy, Mater Sci Eng **32**, 296 (2012).
- [15] S. L. Iconaru, C. S. Ciobanu, P. Le Coustumer, D. Predoi, J Supercond Nov Magn **25**, 2547 (2012).
- [16] D. Predoi, R. A. Vatasescu-Balcan, J. Optoelectron. Adv. Mater. **10**, 152 (2008).
- [17] A. H. Lu, E. L. Salabas, F. Schuth, Angew Chem Int Ed Engl **46**, 1222 (2007).
- [18] D. Predoi, Dig J Nanomater Bios **2**, 169 (2007).
- [19] M. Lewin, N. Carlesso, C. H. Tung, X. W. Tang, D. Cory, D. T. Scadden, R. Weissleder, Nat Biotechnol. **18**, 410 (2000).
- [20] A. Ito, M. Shinkai, H. Honda, T. Kobayashi, J. Biosci. Bioeng. **100**, (2005).
- [21] C. Alexiou, W. Arnold, R. J. Klein, F. G. Parak, P. Hulin, C. Bergemann, W. Erhardt, S. Wagenpfeil, A. S. Lubbe, Cancer Research **60**, 6641 (2000).
- [22] S. Acharya, S. K. Sahoo, Adv Drug Deliv Rev **63**, 170 (2011).
- [23] J. W. M. Bulte, R. A. Brooks, B. M. Moskowitz, Magn. Reson. Med. **42**, 379 (1999).
- [24] R. Massart, IEEE Trans Magn **17**, 1247 (1981).
- [25] C. S. Ciobanu, S. L. Iconaru, E. Gyorgy, M. Radu, M. Costache, A. Dinischiotu, P. Le Coustumer, K. Lafdi, D. Predoi, Chem. Cent. J. **6** (2012).
- [26] D. Predoi, C. M. Valsangiacom, J. Optoelectron. Adv. Mater. **9**, 1797 (2007).
- [27] M. Grumezescu, E. Andronescu, A. Fici, C. Bleotu, M. C. Chifiriuc, Biointerface Research in Applied Chemistry **2**, 446 (2012).
- [28] A. M. Prodan, S. L. Iconaru, C. M. Chifiriuc, C. Bleotu, C. S. Ciobanu, M. Motelica-Heino, S. Sizaret, D. Predoi, J. Nanomater. **2013**, 1 (2013).
- [29] B. Su, S. L. Xiang, J. Su, H. L. Tang, Q. J. Liao, Y. J. Zhou, S. Qi, Biochem. Pharmacol. **1**, 106 (2012).
- [30] A. Pizzoferrato, G. Ciapetti, S. Stea, E. Cenni, C. R. Arciola, D. Granchi, L. Savarino, Clin. Mater. **15**, 173 (1994).
- [31] C. J. Kirkpatrick, F. Bittinger, M. Wagner, H. Köhler, T. G. van Kooten, C. L. Klein, M. Otto, Proc. Inst. Mech. Eng. H. **212**, 75 (1998).
- [32] S. R. Dave, X. Gao, Wiley Interdiscip Rev Nanomed Nanobiotechnol. **1**, 583 (2009).
- [33] J. Sun, S. Zhou, P. Hou, Y. Yang, J. Weng, X. Li, M. Li, J Biomed Mater Res A. **80**, 333 (2007).
- [34] F. Y. Cheng, C. H. Su, Y. S. Yang, C. S. Yeh, C. Y. Tsai, C. L. Wu, M. T. Wu, D. B. Shieh, Biomaterials **26**, 729 (2005).
- [35] J. Emerit, C. Beaumont, F. Trivin, Biomed Pharmacother **55**, 333 (2001).
- [36] Y. Li, J. Liu, Y. Zhong, J. Zhang, Z. Wang, L. Wang, Y. An, M. Lin, Z. Gao, D. Zhang, Int J Nanomedicine **6**, 2805 (2011).
- [37] T. K. Jain, M. K. Reddy, M. A. Morales, D. L. Leslie-Pelecky, V. Labhasetwar, Mol Pharm. **5**, 316 (2008).